

SUPPORTING INFORMATION

Antioxidant deactivation on graphenic nanocarbon surfaces

Xinyuan Liu¹, Sujat Sen¹, Jingyu Liu¹, Indrek Kulaots², David Geohegan⁵, Agnes Kane^{3,4}, Alex A. Puretzky⁵, Christopher M. Rouleau⁵, Karren L. More⁶, G. Tayhas R. Palmore^{1,2,4*}, Robert H. Hurt^{2,4*}

¹Department of Chemistry, ²School of Engineering, ³Department of Pathology and Laboratory Medicine, ⁴Institute for Molecular and Nanoscale Innovation, Brown University, Providence, RI; ⁵Center for Nanophase Materials Sciences, Oak Ridge National Laboratory, Oak Ridge, TN ⁶Shared Research Equipment Facility, Oak Ridge National Laboratory, Oak Ridge, TN

*Corresponding authors: Robert Hurt (Robert_Hurt@brown.edu)

G. Tayhas R. Palmore (Tayhas_Palmore@brown.edu)

A panel of typical morphologies of selected carbon nanomaterials including P-SWNT, single-walled nanohorns, long and short MWCNTs, N-doped MWNTs used in this study is shown in Figure S1 and Figure S2. As-produced, SWNHs are irregularly-shaped, sealed single-walled carbon structures which appear to grow by the self-assembly of graphene fragments and fullerenes during the cooling of the laser plasma. Their wall structure is that of graphene with the incorporation of sufficient structural defects to form somewhat irregular closed structures without observable open edges. As shown in Figure S1b, nanohorns are found within tightly-bound aggregates which have interstitial pore sizes which vary with the size of the individual nanohorns. Although the TEM images reveal the internal pores of the SWNHs in the aggregate, these pores are inaccessible until they are opened by oxidative treatments. Moreover, the tight packing of SWNHs provides only sub-nm interstitial pores which do not permit the adsorption of H₂ at 77K.^[1]

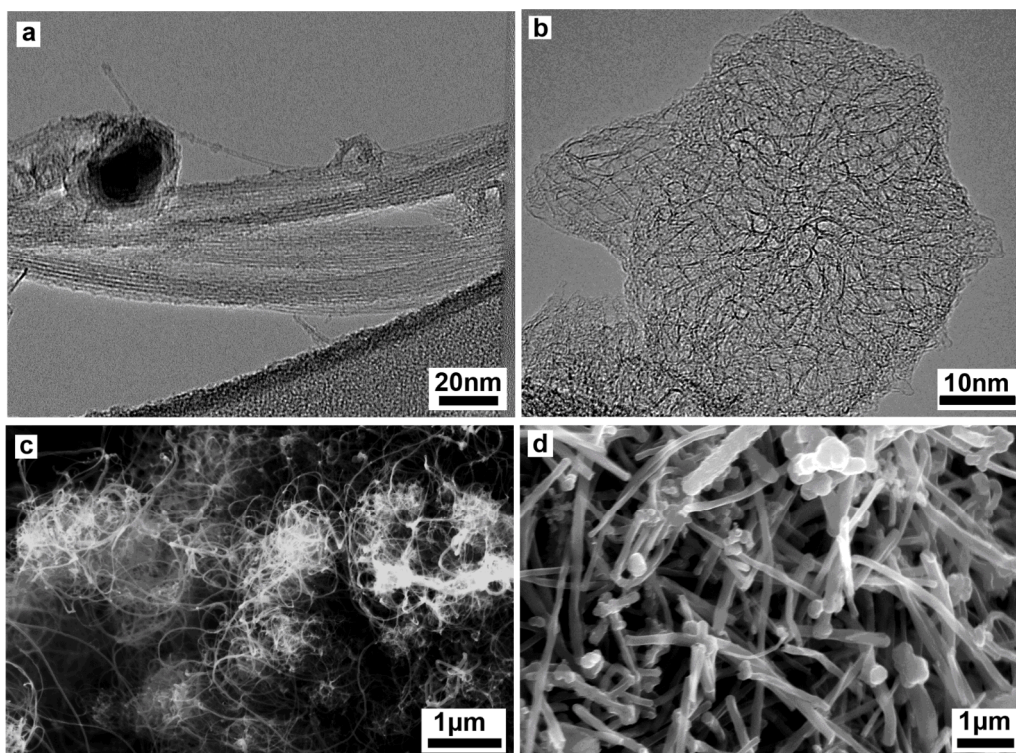


Figure S1. Morphologies of selected graphenic nanomaterials in Fig. 5. (a) P SWNT, (b) carbon nanohorns, (c) MWNT-1, (d) MWNT-2.

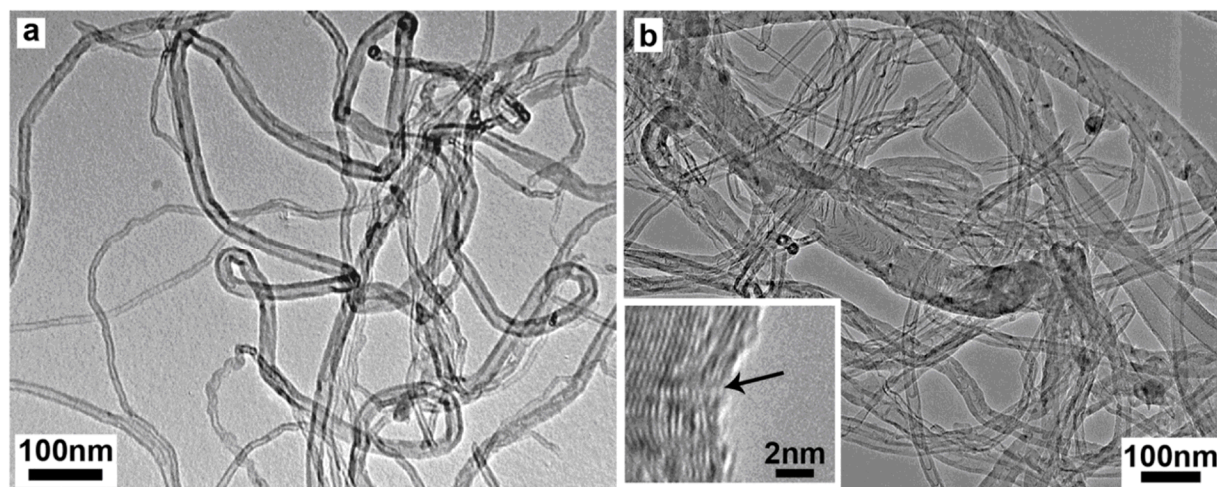


Figure S2. Comparative morphologies of MWNTs (left) and N-doped MWNTs (right) with higher GSH oxidation activity. MWNTs and N-doped MWNTs show similar diameter and morphology but N-doped MWNTs have a bamboo structure with potentially higher densities of graphene edge sites on the sidewalls (b inset).

N-acetylcysteine (NAC) is a thiol-containing amino acid, and SWNTs depleted NAC instead of GSH when both are present in our system (Fig. S3), since NADPH and GR can only reduce oxidized GSH but not NAC once it is oxidized. It is reported that the relative reactivity of different thiol compounds with hydrogen peroxide and superoxide was inversely related to the pK of the thiol group.^[2] The pK value of GSH is 8.8, which is lower than that of N-acetylcysteine (9.5), indicating that GSH is more reactive than NAC towards oxidation by hydrogen peroxide and superoxide.^[2] However, in our study NAC showed a striking higher reactivity with carbon nanotubes than GSH, considering GSH has a relatively higher steric effect than NAC, which may suggest a reaction associated with carbon nanotube surface. Figure 4.5c and d demonstrate that GSH can be regenerated by a reducing reagent.

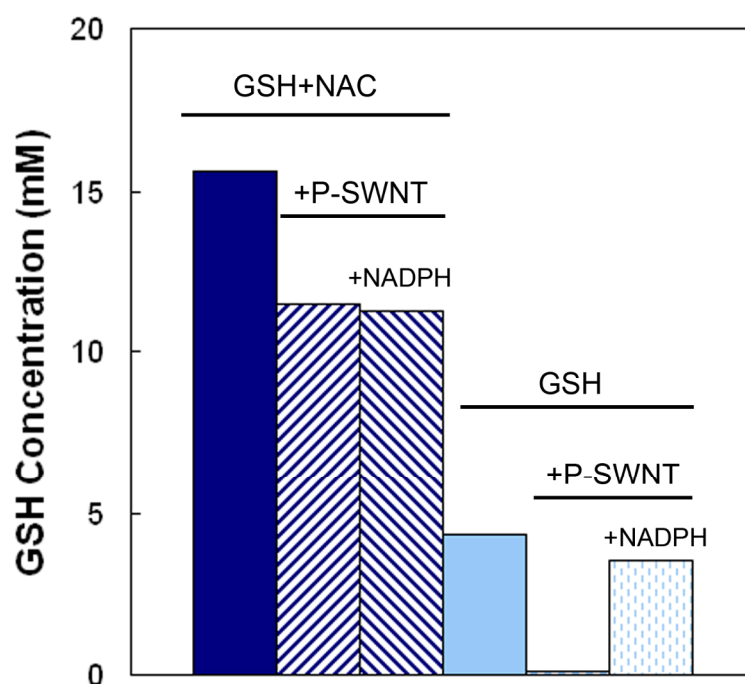


Figure S3. Relative reactivity of GSH and N-acetylcysteine (NAC) as a probe for steric effects in the SWNT-mediated GSH-O₂ reaction. NAC disappears preferentially to GSH, and its higher reactivity suggests steric effects in the thiol-ROS step, consistent with surface bound ROS.

Figure S4 demonstrates that severe oxidation of SWNTs with H₂SO₄/HNO₃ eliminated the GSH activity presumably by functionalizing the catalytic active sites.

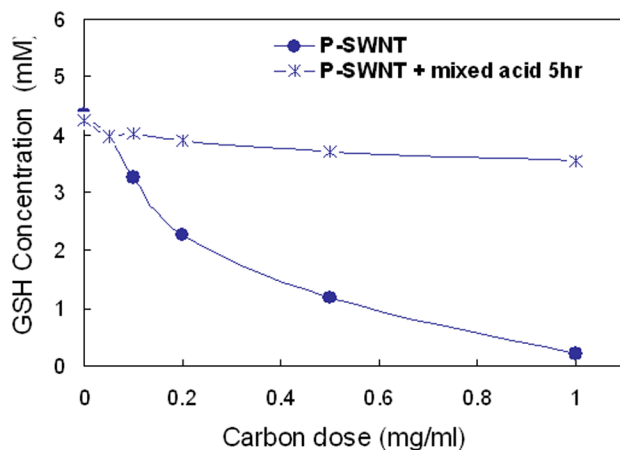


Figure S4. Effect of extreme H₂SO₄/HNO₃ oxidation on the GSH activity of SWNTs. 5-hr acid oxidation converts the SWNT to hydrophilic carbonaceous debris, which has a low GSH activity.

Another concern of the oxidation of GSH may be raised from bioavailable metal residuals in carbon nanomaterials or any trace bioavailable metal in nanopure water that can produce ROS and result in GSH oxidation. Figure 5S show that there is no significant difference of GSH reactivity after removal of those possible bioavailable metal ions by 3M HCl purification or chelexing and filtering the PBS buffer, indicating that the catalytic effects are not due to trace metals in PBS, nor to dissolvable trace metal on the surfaces of SWNTs or carbon black.

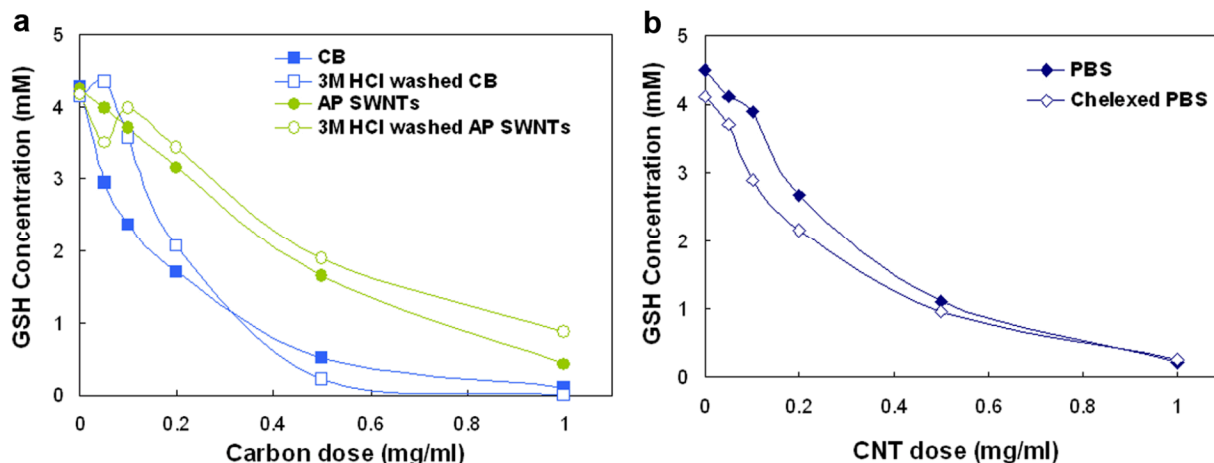


Figure S5. Test for metals effect in the redox activity of SWNTs and carbon black. The data suggest the primary sources of redox activity in these two samples are carbon-based active sites.

Supporting References

1. D. B. Geohegan, A. A. Puretzky, C. M. Rouleau, M. Yoon, N. Thonnard, K. L. More, G. Duscher, Proceedings of the 2010 Annual Merit Review Hydrogen Program Sorption Center of Excellence, available online at http://www.hydrogen.energy.gov/pdfs/review10/st017_geohegan_2010_p_web.pdf.
2. C. C. Winterbourn, D. Metodiewa, *Free Radical Bio. Med.* **1999**, 27, 322-328.